

would also give an A_2X pattern; however, the NMR data for the mixed-anion complexes and conductance data (vide supra) rule this out. Hypothetically, upon addition of excess ligand L to L_2PtCl_2 and to L_2PtBr_2 , we could possibly observe L_3PtCl_2 , L_3PtBr_2 , $[L_3PtCl]^+Cl^-$, or $[L_3PtBr]^+Br^-$. Similarly, we would expect the addition of L to $L_2PtClBr$ to give $L_3PtClBr$, $[L_3PtCl]^+Br^-$, or $[L_3PtBr]^+Cl^-$. These last two forms would give $^{31}P\{^1H\}$ and $^{195}Pt\{^1H\}$ NMR spectra essentially identical with those for the dichloro and dibromo species, if ionic compounds were being formed in these cases. The results in Table VII exclude the possibility of ionic complexes as the NMR spectra of $L_2PtClBr + L$ are substantially different from those of either $L_2PtCl_2 + L$ or $L_2PtBr_2 + L$. NMR spectroscopy alone cannot unambiguously determine the geometry of L_3MX_2 species in solution, since the same A_2X pattern is expected for each of the four configurations (Figure 8). The solution geometries of the complexes are most likely distorted between SBP and TBP, consistent with the limited amount of structural data⁴⁴ for L_3MX_2 complexes.

Acknowledgment. The financial support of the University of Nevada, Reno, Research Advisory Board is gratefully acknowledged. We are grateful to the National Science Foundation (Grant No. CHE77-08937) for providing funds to purchase the Fourier transform NMR spectrometer. Helpful

discussions with Professor H. E. LeMay are greatly appreciated.

Registry No. *cis*- L_2PtX_2 , R = CH₃, X = Cl, 81011-50-9; *cis*- L_2PtX_2 , R = *n*-Bu, X = Cl, 81011-51-0; *cis*- L_2PtX_2 , R = *t*-Bu, X = Cl, 81011-52-1; *cis*- L_2PtX_2 , R = Bzl, X = Cl, 81011-53-2; *cis*- L_2PtX_2 , R = Ph, X = Cl, 81011-54-3; *cis*- L_2PtX_2 , R = CH₃, X = Br, 81011-55-4; *cis*- L_2PtX_2 , R = *n*-Bu, X = Br, 81011-56-5; *cis*- L_2PtX_2 , R = *t*-Bu, X = Br, 81011-57-6; *cis*- L_2PtX_2 , R = Bzl, X = Br, 81011-58-7; *cis*- L_2PtX_2 , R = Ph, X = Br, 81027-52-3; *cis*- L_2PtX_2 , R = CH₃, X = I, 81011-59-8; *trans*- L_2PtX_2 , R = CH₃, X = I, 81075-66-3; *cis*- L_2PtX_2 , R = *n*-Bu, X = I, 81011-60-1; *trans*- L_2PtX_2 , R = *n*-Bu, X = I, 81011-61-2; *cis*- L_2PtX_2 , R = *t*-Bu, X = I, 81075-67-4; *cis*- L_2PtX_2 , R = Bzl, X = I, 81011-62-3; *trans*- L_2PtX_2 , R = Bzl, X = I, 81075-68-5; *cis*- L_2PtX_2 , R = Ph, X = I, 81011-63-4; *cis*- $L_2PtBrCl$, R = CH₃, 81011-64-5; *cis*- $L_2PtBrCl$, R = *n*-Bu, 81011-65-6; *cis*- $L_2PtBrCl$, R = *t*-Bu, 81011-66-7; *cis*- $L_2PtBrCl$, R = Ph, 81011-67-8; *cis*- $L_2PtBrCl$, R = Bzl, 81011-68-9; $L_3PtBrCl$, R = CH₃, 81011-69-0; $L_3PtBrCl$, R = *n*-Bu, 81011-70-3; $L_3PtBrCl$, R = *t*-Bu, 81011-71-4; $L_3PtBrCl$, R = Ph, 81011-72-5; $L_3PtBrCl$, R = Bzl, 81011-73-6; L_3PtCl_2 , R = *t*-Bu, 81011-74-7; *cis*- L_2PtX_2 , L = Bzl₃P, X = Cl, 81075-69-6; *trans*- L_2PtX_2 , L = Bzl₃P, X = Cl, 63902-66-9; *trans*- L_2PtX_2 , L = Bzl₂PhP, X = Cl, 63848-36-2; *cis*- L_2PtX_2 , L = BzlPh₂P, X = Cl, 61586-06-9; *cis*- L_2PtX_2 , L = Bu₃P, X = Cl, 15390-92-8; *cis*- L_2PtX_2 , L = Et₃P, X = Cl, 15692-07-6; *trans*- L_2PtX_2 , L = Et₃P, X = Cl, 13965-02-1; *cis*- L_2PtX_2 , L = Me₃P, X = Cl, 15630-86-1; *cis*- L_2PtX_2 , L = Me₂PhP, X = Cl, 15393-14-3; *cis*- L_2PtX_2 , L = Me₂PhP, X = Br, 15616-81-6; *cis*- L_2PtX_2 , L = Me₂PhP, X = I, 41119-52-2; *trans*- L_2PtX_2 , L = Me₂PhP, X = I, 4119-53-3; *cis*- L_2PtX_2 , L = MePh₂P, X = Cl, 16633-72-0; *cis*- L_2PtX_2 , L = MePh₂P, X = Br, 52613-13-5; *cis*- L_2PtX_2 , L = MePh₂P, X = I, 28425-03-8; *trans*- L_2PtX_2 , L = MePh₂P, X = I, 28425-02-7.

(44) Louw, W. J.; deWaal, D. J. A.; Kruger, G. J. *J. Chem. Soc., Dalton Trans.* 1976, 2364. Chui, K. M.; Powell, H. M. *Ibid.* 1974, 2117. Chui, K. M.; Powell, H. M. *Ibid.* 1974, 1879.

Contribution from the Kenan Laboratories of Chemistry, The University of North Carolina, Chapel Hill, North Carolina 27514

Electropolymerization of Vinylpyridine and Vinylbipyridine Complexes of Iron and Ruthenium: Homopolymers, Copolymers, Reactive Polymers

P. DENISEVICH, H. D. ABRUÑA, C. R. LEIDNER, T. J. MEYER,* and ROYCE W. MURRAY*

Received July 10, 1981

Electroreductive polymerizations of the vinyl-substituted monomer complexes $[Ru(vbpy)_3]^{2+}$, $[Fe(vbpy)_3]^{2+}$, $[Ru(bpy)_2(vpy)_2]^{2+}$, $[Ru(bpy)_2(vpy)Cl]^+$, $[Ru(vbpy)_2Cl_2]$, $[Ru(bpy)_2(vpy)NO_2]^+$, and $[Ru(bpy)_2(vbpy)]^{2+}$ are described, where *vbpy* = 4-vinyl-4'-methyl-2,2'-bipyridine and *vpy* = 4-vinylpyridine. The polymers form stable, adherent, electrochemically reactive films on the reducing electrode, which can be Pt, Au, vitreous carbon, SnO₂, or TiO₂. Complexes with only one vinyl substituent are difficult to polymerize but can be copolymerized with divinyl- and trivinyl-substituted monomers. The possibility that the polymers are in part metal macroclusters with bridging ligands is discussed. Films containing from 4 to ca. 1500 monolayers of metal complex can be formed depending on the potential control conditions employed during polymerization. Charge transport through poly- $[Ru(vbpy)_3]^{2+}$ films occurs with $D_{et} = 2 \times 10^{-10}$ cm²/s, which corresponds to an apparent $[Ru(vbpy)_3]^{3+/2+}$ electron-self-exchange rate in the film of 1.7×10^5 M⁻¹ s⁻¹. Quantitative reactivity of ruthenium centers in this film was demonstrated with use of spectrophotometry of films on SnO₂ electrodes, and composition was evaluated by X-ray photoelectron spectroscopy. The cross-linked, polycationic films are poorly permeable to cations and bulky, neutral molecules dissolved in the contacting solution but readily incorporate small anions. Chemical reactivity of poly- $[Ru(bpy)_2(vpy)NO_2]^+$ is somewhat altered by the polymeric environment as compared to that of prior monolayer studies.

Binding of transition-metal complexes to preformed, ligand-containing polymers^{1,2} typically results, for steric and/or electrostatic reasons, in incomplete metalation of the polymeric ligand sites. This has been the case in recent studies involving the coating of electrodes with cobalt and ruthenium complexes bound to polyvinylpyridine.^{2b,3-7}

We recently described⁸ the coating of electrodes by the reductive, electrochemical polymerization of several vinylpyridine and vinylbipyridine complexes of iron and ruthenium. The use of vinyl-substituted metal complexes as monomers offers the possibility of preparing polymeric films with essentially complete metalation of ligand sites and a well-defined coordination environment for the metal. Since the monomer metal complex approach to electroactive polymer films is uncommon, we have carried out studies aimed at better understanding the ruthenium vinylpyridine and vinylbipyridine electropolymerizations and the possible generality of the chemistry involved. These studies have included relative ease

- (1) Tsuchida, E.; Nischide, H. *Adv. Polym. Sci.* 1977, 24, 1.
- (2) (a) Oyama, N.; Anson, F. C. *J. Am. Chem. Soc.* 1979, 101, 739. (b) *Ibid.* 1979, 101, 3450.
- (3) Oyama, N.; Anson, F. C. *J. Electrochem. Soc.* 1980, 127, 247.
- (4) Oyama, N.; Shimomura, T.; Shigehara, K.; Anson, F. C. *J. Electroanal. Chem. Interfacial Electrochem.* 1980, 112, 271.
- (5) Haas, O.; Vos, J. G. *J. Electroanal. Chem. Interfacial Electrochem.* 1980, 113, 139.
- (6) Calvert, J.; Meyer, T. J. *Inorg. Chem.* 1981, 20, 27.
- (7) Samuels, G. J.; Meyer, T. J. *J. Am. Chem. Soc.* 1981, 103, 307.

- (8) Abruña, H. D.; Denisevich, P.; Umaña, M.; Meyer, T. J.; Murray, R. W. *J. Am. Chem. Soc.* 1981, 103, 1.

of polymerization of monomers with different numbers of vinyl groups, the analytical composition of the polymer films, their electrochemistry, and the rate at which electrochemical charge diffuses through one of the films. The metal complex monomers used in this paper are $[\text{Ru}(\text{vbpy})_3]^{2+}$, $[\text{Fe}(\text{vbpy})_3]^{2+}$, $[\text{Ru}(\text{vbpy})_2\text{Cl}_2]$, $[\text{Ru}(\text{bpy})_2(\text{vpy})_2]^{2+}$, $[\text{Ru}(\text{bpy})_2(\text{vbpy})]^{2+}$, $[\text{Ru}(\text{bpy})_2(\text{vpy})\text{Cl}]^{2+}$, and $[\text{Ru}(\text{bpy})_2(\text{vpy})\text{NO}_2]^+$, where vbpy is 4-vinyl-4'-methyl-2,2'-bipyridine, vpy is 4-vinylpyridine, and bpy is 2,2'-bipyridine. Results are presented to suggest that the polymer structure may in part be composed of metal macroclusters with bridging ligands as opposed to simply long strands of polymeric ligands chains with metal complexes dangling therefrom.

Experimental Section

Chemicals. The ligand 4-vinyl-4'-methyl-2,2'-bipyridine (vbpy) and the ruthenium and iron complexes $[\text{Ru}(\text{vbpy})_3](\text{PF}_6)_2$, $[\text{Fe}(\text{vbpy})_3](\text{PF}_6)_2$, $[\text{Ru}(\text{bpy})_2(\text{vpy})_2](\text{ClO}_4)_2$, and $[\text{Ru}(\text{bpy})_2(\text{vpy})\text{Cl}](\text{ClO}_4)$ were prepared as previously described.⁸

$[\text{Ru}(\text{bpy})_2(\text{vpy})\text{NO}_2](\text{PF}_6)$ was prepared by a different procedure than that reported⁹ for the corresponding pyridine complex. A deaerated 1/1 (v/v) water/ethanol solution of *cis*- $\text{Ru}(\text{bpy})_2\text{Cl}_2 \cdot 2\text{H}_2\text{O}$ containing a 20% molar excess of vinylpyridine was heated at reflux for 45 min under N_2 . A 20% molar excess of NaNO_2 was added to the cooled reaction mixture, which was then heated further at reflux for 3 h. After cooling, the reaction mixture was reduced to half the initial volume and refrigerated overnight. The cooled solution was filtered to remove a red precipitate, presumably $\text{Ru}(\text{bpy})_2(\text{NO}_2)_2$, and the desired complex was precipitated from the filtrate by addition of 2 mL of saturated aqueous NH_4PF_6 . The precipitate was collected, washed with water and ether, and dried in vacuo at 50 °C overnight. The solid was purified by dissolving in a minimum quantity of acetonitrile and reprecipitating with ether.

Electrochemical solvents were obtained from Burdick and Jackson and were stored over 4A molecular sieves. Tetraethylammonium perchlorate supporting electrolyte was thrice recrystallized from water.

Electrochemical Polymerization. A clean electrode was placed in a dilute (0.1–0.5 mM) solution of the appropriate monomer containing, typically, 0.1 M supporting electrolyte. After the solution was degassed with a nitrogen stream, the electrode potential was repetitively swept between 0 and, except as noted elsewhere, –1.8 V vs. SSCE. Progress of the deposition was monitored by the growth of the bpy reduction waves of the complexes in the polymer film, between –1.3 and –1.8 V.

The more difficultly polymerized monomers (see text) were generally deposited potentiostatically in unstirred solution. The use of higher monomer concentrations or of stirred solutions resulted in more rapid polymerization and, generally, in formation of thick, fragile films.

Cells and Equipment. Conventional three-electrode cells and potential control circuits were employed throughout. NaCl-saturated SCE (SSCE) was used as reference electrode. X-ray photoelectron spectroscopy was carried out with use of Du Pont Model 650B and PHI Model 548AR electron spectrometers.

Results and Discussion

Polymerization and Electrochemistry of $[\text{Ru}(\text{vbpy})_3]^{2+}$, $[\text{Fe}(\text{vbpy})_3]^{2+}$, and $[\text{Ru}(\text{bpy})_2(\text{vpy})_2]^{2+}$. When a clean Pt electrode is placed in a degassed solution of $[\text{Ru}(\text{vbpy})_3]^{2+}$ in 0.1 M $\text{Et}_4\text{NClO}_4/\text{CH}_3\text{CN}$ and the potential scanned repeatedly between 0 or –1.0 and –1.8 V vs SSCE, the electrochemical waves for the $[\text{Ru}(\text{vbpy})_3]^{2+/1+}$ and $[\text{Ru}(\text{vbpy})_3]^{1+/0}$ couples appearing at –1.45 and –1.54 V respectively, gradually and continually increase in size (Figure 1A). Currents on the first potential cycle are quite small since the concentration of $[\text{Ru}(\text{vbpy})_3]^{2+}$, 0.1 mM, diffusing to the electrode surface is small but subsequently become much larger than accountable by diffusion-controlled electrochemistry. Deposition of a film of a polymeric, electroactive form of the complex, poly- $[\text{Ru}(\text{vbpy})_3]^{2+}$, on the electrode surface, which gives rise to the larger currents, is demonstrated by transferring the Pt

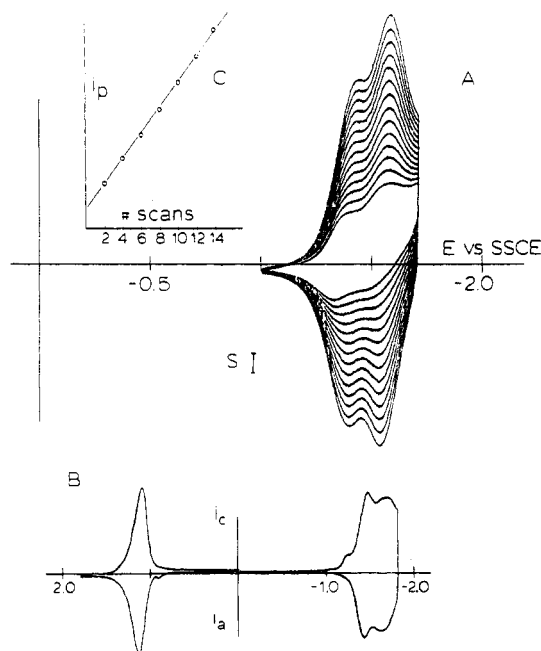


Figure 1. Curve A: reductive electropolymerization of $[\text{Ru}(\text{vbpy})_3]^{2+}$ on a Pt electrode by repeated potential scans at 100 mV/s between –1.0 and –1.7 V vs. SSCE in 0.1 $\text{Et}_4\text{NClO}_4/\text{CH}_3\text{CN}$ containing 0.1 mM $[\text{Ru}(\text{vbpy})_3]^{2+}$. Increasing waves represent growth of film. The number of scans is indicated on the figure. Curve B: cyclic voltammetry of above electrode at 200 mV/s, in clean 0.1 M $\text{Et}_4\text{NClO}_4/\text{CH}_3\text{CN}$. $\Gamma = 1 \times 10^{-9}$ mol/cm². $S = 75$ and $180 \mu\text{A}/\text{cm}^2$ for curves $\mu\text{A}/\text{cm}^2$ A and B. Curve C: peak currents as a function of number of scans for the electrode of curve A during electropolymerization.

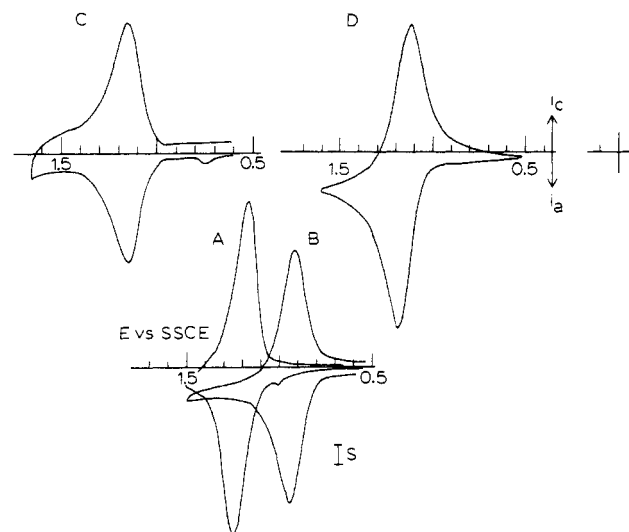


Figure 2. Cyclic voltammetry in 0.1 M $\text{Et}_4\text{NClO}_4/\text{CH}_3\text{CN}$ in the $\text{Ru}^{\text{III/II}}$ region for films on Pt of the following: curve A, 1.2×10^{-8} mol/cm² poly- $[\text{Ru}(\text{bpy})_2(\text{vpy})_2]^{2+}$, 200 mV/s; curve B, 1.2×10^{-9} mol/cm² poly- $[\text{Fe}(\text{vbpy})_3]^{2+}$, 200 mV/s; curve C, 6.1×10^{-10} mol/cm² poly- $[\text{Ru}(\text{vbpy})_3]^{2+}$, 200 mV/s; curve D, 1.3×10^{-7} mol/cm² poly- $[\text{Ru}(\text{vbpy})_3]^{2+}$, 5 mV/s. $S = 250, 25, 1,$ and $50 \mu\text{A}/\text{cm}^2$ for curves A–D, respectively.

electrode, after thorough rinsing, to clean supporting electrolyte solution, whereupon the $[\text{Ru}(\text{vbpy})_3]^{2+/1+}$ and $[\text{Ru}(\text{vbpy})_3]^{1+/0}$ reduction waves and the $[\text{Ru}(\text{vbpy})_3]^{3+/2+}$ oxidation wave (Figure 1B) remain observable. Similar results are obtained with the complexes $[\text{Ru}(\text{bpy})_2(\text{vpy})_2]^{2+}$ and $[\text{Fe}(\text{vbpy})_3]^{2+}$; Figure 2A and B shows the $\text{M}^{\text{III/II}}$ waves for their polymeric films in clean supporting electrolyte (0.1 M $\text{Et}_4\text{NClO}_4/\text{CH}_3\text{CN}$). In these and other cases discussed below, the formal potentials $E^{\circ'}$ for the polymeric films are close to those for

(9) Abrufu, H. D. Ph.D. Thesis, The University of North Carolina, Chapel Hill, NC, 1980.

Table I. Electrochemical Data (Volts) for Ruthenium Complexes Bearing Vinylpyridine or Vinylbipyridine Ligands (in 0.1 M $\text{Et}_4\text{NClO}_4/\text{CH}_3\text{CN}$)

complex	soln			polymer films		
	E°_{ox}	$E^{\circ}_{\text{red}(1)}$	$E^{\circ}_{\text{red}(2)}$	E°_{ox}	$E^{\circ}_{\text{red}(1)}$	$E^{\circ}_{\text{red}(2)}$
$[\text{Ru}(\text{bpy})_2(\text{vpy})_2]^{2+}$	1.24	-1.35 _s	-1.55	1.22 _s	-1.36	-1.52
$[\text{Ru}(\text{bpy})_2(\text{vpy})\text{Cl}]^+$	0.76	-1.49	-1.74 ^a	0.76	-1.48	...
$[\text{Ru}(\text{bpy})_2(\text{vpy})\text{NO}_2]^+$	1.03 ^b	-1.45 _s	-1.69	1.03 ^b
$[\text{Ru}(\text{bpy})_2(\text{vpy})\text{NO}_3]^+$	0.96 ^c	0.91
$[\text{Ru}(\text{bpy})_2(\text{vpy})\text{NO}]^{3+}$	0.53 ^c	0.47
$[\text{Ru}(\text{vbpy})_3]^{2+}$	1.16	-1.43	-1.54	1.16	-1.43	-1.54
$[\text{Fe}(\text{vbpy})_3]^{2+}$	0.93 _s	-1.42	-1.58	0.93	-1.44	-1.57
$[\text{Ru}(\text{vbpy})_3]^{2+}$	0.925 ^e
$[\text{Ru}(\text{bpy})_2(\text{vpy})_2]^{2+}$	1.045 ^e
$[\text{Ru}(\text{vbpy})_2\text{Cl}_2]$	0.30	0.36
$[\text{Ru}(\text{bpy})_2(\text{MeCN})\text{vpy}]^{2+}$	1.36 ^c	1.29
$[\text{Ru}(\text{vbpy})_2(\text{MeCN})_2]^{2+}$	1.41 ^d	1.35

^a E_{pc} . ^b E_{pa} . ^c Value for the py complex in solution. ^d Value for the bpy complex in solution. ^e In 1 M HClO_4 .

the dissolved complexes (Table I).

Formation of these adherent films requires⁸ the presence of the vinyl groups on the ligands (no accumulation occurs for reduction of $[\text{Ru}(\text{bpy})_3]^{2+}$) as well as reduction of the complex. Films can be prepared on Au, vitreous carbon, SnO_2 , and TiO_2 electrodes with use of much the same procedure as above.

Many more electroactive sites are present in the films (coverage Γ mol/cm² measured by integrating the charge under the $\text{M}^{\text{III/II}}$ waves) than in a monomolecular layer¹⁰ (ca. 8×10^{-11} mol/cm²) of these complexes. The coverage of deposited polymer can be readily and reproducibly adjusted by varying the number of cyclical potential scans and sweep rate. For example, three $0 \rightarrow -1.8 \rightarrow 0$ V potential cycles (at 0.1 V/s) suffice to deposit 5×10^{-10} mol/cm² of electroactive polymer from a 0.5 mM $[\text{Ru}(\text{vbpy})_3]^{2+}$ solution whereas 90 min of scanning (150 scans) yields a coverage of 5×10^{-7} mol/cm². Under fixed conditions, the increment of polymer per scan is approximately constant as shown by Figure 1C.

Polymerization also proceeds by using potential scans through only the first $[\text{Ru}(\text{vbpy})_3]^{2+}$ reduction wave, but films accumulate more slowly (by ca. 10 times). Higher concentrations of monomer or stirring of the solution accelerates buildup of the film. If the deposition is carried out too rapidly or for too long, very thick films ($>10^{-6}$ mol/cm²) are formed that are visibly rough and mechanically fragile and can be dislodged by a stream of solvent (wash bottle). (The thinner films are in contrast very adherent and stable to vigorous washing.) Finally, while film growth is most conveniently monitored by repeatedly scanning the electrode potential, deposition can also be carried out potentiostatically. While we have not detected substantive differences in the electrochemistry of potential scanning and potentiostatically deposited films, in view of the repeated halting of the polymerization, which presumably occurs with the scanning procedure, some structural differences in the polymer may nonetheless exist.

Films of poly- $[\text{Ru}(\text{vbpy})_3]^{2+}$, poly- $[\text{Fe}(\text{vbpy})_3]^{2+}$, and poly- $[\text{Ru}(\text{bpy})_2(\text{vpy})_2]^{2+}$ deposited on mirror-smooth Pt vary in appearance depending on coverage. For $\Gamma \leq 10^{-8}$ mol/cm², the electrode surface retains its metallic luster and ranges in color from very pale yellow to bright orange (for Ru) and from pale pink to violet (for Fe). The colorations are due to optical absorbances and not to interference phenomena. Thicker films gradually become opaque and have a roughened surface. On electrodes with thick coatings, some of the orange polymer often extends beyond the edge of the Pt disk onto the Teflon collar for 1–2 mm. This could result from adsorption of oligomers onto the Teflon from the solution around the electrode or from an extension of polymer chains from the Pt edge.

The former possibility is considered more plausible, and if so, proper flow and electrode arrangements may permit controlled deposition of polymer films on nonconducting surfaces. (The edge buildup possibility is mentioned because the sensitivity of polymer growth rate to concentration might couple with the high electrode-edge mass-transport rate (nonlinear diffusion) to accelerate polymer growth there. Additionally, uniformity of deposition is best when the cell geometry favors uniform current distribution. If the reference and auxiliary electrodes are displaced to one side of the Pt disk, film buildup on Pt and Teflon collar tends to become accentuated on that side.) In view of the estimated rates of charge transport through these films (vide infra) and the physical distances involved (1–2 mm), it is unlikely that polymer deposited on the Teflon collar is significantly involved in electrochemical experiments on the cyclic voltammetric time scale.

A sample of $[\text{poly-}[\text{Ru}(\text{bpy})_2(\text{vpy})_2]](\text{ClO}_4)_2$, mechanically dislodged from a film grown to excessive thickness, gave⁸ an elemental analysis close to that anticipated for maintenance of the original monomer coordination sphere. This supports our view of these films as polymeric forms of intact metal complex monomers. The polymers are intractably insoluble in all media tested (water, acids, concentrated HNO_3 , acetone, DMF, Me_2SO , CH_2Cl_2), so other analytical characterizations have been limited to the intact films. These include the following: (i) Formal potentials of the surface waves for the polymeric complexes are consistently close to those of the dissolved complexes (Table I). In view of the sensitivity of $\text{Ru}^{\text{III/II}}$ formal potentials to the ligands,¹¹ this is significant evidence for integrity of the monomer coordination following polymerization. For some monomers, coordinative changes do occur upon polymerization, which can be detected through the $\text{Ru}^{\text{III/II}}$ formal potentials (vide infra). (ii) X-ray photoelectron spectroscopy (XPS) of films of $[\text{poly-}[\text{Ru}(\text{bpy})_2(\text{vpy})_2]](\text{ClO}_4)_2$ shows bands at binding energies Ru 3d_{5/2} (280.5 eV), N 1s (398.6 eV), and Cl 2p (206.9 eV). The relative (integrated) intensities indicate Ru/N/Cl atom ratios of 1/8.3/2.9. The high ratios of N and Cl to Ru may result from two factors: possible Et_4NClO_4 electrolyte trapped in the polymer and/or low accuracy in measuring the intensity of the Ru 3d_{5/2} band, which slightly overlaps the C 1s band. (iii) Evidence of the anion-exchange character expected for a fixed-cation-site film comes from experiments on dissolved redox couple permeation (vide infra). (iv) Resonance Raman spectra of poly- $[\text{Ru}(\text{vbpy})_3]^{2+}$ films show¹² the expected pattern of bipyridine vibrations. (v) A visible spectrum of a poly- $[\text{Ru}(\text{bpy})_2(\text{vpy})_2]^{2+}$ film deposited⁸ on n-SnO₂ has a

(10) Abruña, H. D.; Meyer, T. J.; Murray, R. W. *Inorg. Chem.* **1979**, *18*, 3233.

(11) Salmon, D. Ph.D. Thesis, The University of North Carolina, Chapel Hill, NC, 1977.

(12) Pemberton, J.; The University of North Carolina, unpublished results.

similar shape, and λ_{\max} (438 nm) is only slightly red shifted from that observed for an acetonitrile solution of the monomer (432 nm). (vi) A spectrum of a poly-[Ru(vbpy)₃]²⁺ film on SnO₂ had¹³ an absorbance of 0.21 A at $\lambda_{\max} = 470$ nm (monomer $\lambda_{\max} = 468$ nm). With the assumption that ϵ for the monomer (1.42×10^4) and for the polymer are the same, this absorbance corresponds to a coverage of 1.5×10^{-8} mol/cm², which agrees with the coverage 1.3×10^{-8} mol/cm² obtained from the cyclic voltammetry of this electrode over the same area. Most if not all of the ruthenium sites present on the electrode thus participate in electrochemical reactions of the film, a somewhat remarkable result considering that this film contains ca. 162 monomolecular layers of monomer sites.

The above results are consistent with a polymer composed of predominantly intact units having the original monomer coordination sphere. There is however charge-trapping evidence (vide infra) that repeated reduction of the film leads to a small (5–10%) population of reductively altered complex. Some of this impurity is probably formed during the reductive polymerization procedure and thus is present even in freshly prepared films. Also, we have examined¹⁴ thin films (2×10^{-10} and 5×10^{-10} mol/cm²) of poly-Ru(vbpy)₃²⁺ deposited on smooth Pt foil by variable-angle XPS in an attempt to measure the film thickness. On the basis of a bulk [poly-[Ru(vbpy)₃]](ClO₄)₂ density of 1.35 g/cm³, the XPS results gave thicknesses of $d_{\text{XPS}} = 34$ and 77 Å, considerably larger than those calculated from electrochemical coverage data, $d_{\text{ec}} = 3$ and 33 Å. Inasmuch as d_{ec} depends inversely on the density used in the calculation, while d_{XPS} is relatively insensitive to density,¹⁵ and since we considered it possible that the density of a very thin film of this polymer might be lower than that of a comparatively massive sample, calculations were performed with the assumption of lower densities for the film. If a value of 0.3 g/cm³ is assumed, d_{ec} (59 and 148 Å) and d_{XPS} (58 and 132 Å) come into good agreement. Other possible explanations, besides film density, did not seem viable.¹⁴ This low density may not, however, persist in polymer buildup more remote from the Pt surface, and so film densities of the higher coverage electrodes used in this paper are probably much closer to that of the 1.35 g/cm³ bulk sample (made by growing an excessively thick, mechanically dislodged film).

Electrodes coated with films of poly-[Ru(vbpy)₃]²⁺, poly-[Fe(vbpy)₃]²⁺, and poly-[Ru(bpy)₂(vpy)]²⁺ are quite stable. In CH₃CN solvent, there is little or no change in the M^{III/II} wave after several hours of continuous potential cycling between 0 and +1.6 V vs SSCE at 100 mV/s (e.g., for 5 h of cycling this is > 550 turnovers and ~94 min as the M^{III} complex). Degradation occurs more rapidly if the potential is extended into the M^{II/I} and M^{I/0} reduction waves. Coated electrodes can be stored for several weeks in air provided care is taken to avoid mechanical injury to the thin films. Except for the very thick deposits, the films easily tolerate vigorous solvent flow and prolonged soaking in common solvents. They are not effectively removed by chemical treatments, and electrodes are best cleaned for reuse by mechanical polishing.

In aqueous acid (1 M HClO₄), electrodes coated with poly-[Ru(vbpy)₃]²⁺ and poly-[Ru(bpy)₂(vpy)]²⁺ films are stable to prolonged soaking and to repeated potential cycling through the Ru^{III/II} wave (no change after 60 min between 0 and +1.35 V at 0.1 V/s). As shown in Figure 3 (by a solid line), cyclic voltammograms of Pt/poly-[Ru(vbpy)₃]²⁺ electrodes in 1 M HClO₄ are roughly additive overlays of the

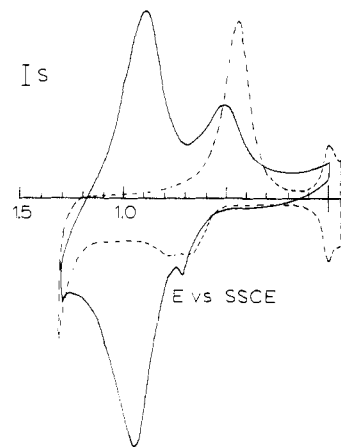


Figure 3. Cyclic voltammetry at 100 mV/s in 1 M HClO₄ of a film of 2×10^{-8} mol/cm² poly-[Ru(vbpy)₃]²⁺ on Pt (solid line) and of naked Pt (dashed line). $S = 100 \mu\text{A}/\text{cm}^2$.

Ru^{III/II} wave and the platinum oxide forming and stripping waves (shown by a dashed line), but the hydrogen adsorption waves of the Pt are blocked by the polymer film. The continued presence of the platinum oxide waves on the coated electrode suggests that interactions between the polymers and the Pt are relatively weak and that the films adhere to the electrode primarily by their insolubility plus perhaps topological molding to the microscopic contours of the Pt surface. Cyclic voltammograms of Pt/poly-[Ru(vbpy)₃]²⁺ electrodes in 1 M H₂SO₄ have an initial appearance⁸ similar to that of Figure 3. Cycling between 0 and +1.3 V vs. SSCE in this case or in pH 5 Na₂SO₄ electrolyte causes a slow decrease in the size of the Ru^{III/II} wave. This decay is associated with the Ru^{III} state and is first order with rate constant ca. $5 \times 10^{-4} \text{ s}^{-1}$. (Decay of Ru^{III} electrodes in 1 M HClO₄ has not been measured but is at least 100 times slower.) Decay in sulfate medium for [Ru(bpy)₃]²⁺ electrostatically trapped in Nafion membranes is reported to be partially reversed by overnight soaking.¹⁶ We have also found that soaking or prolonged potential cycling of Pt/poly-[Ru(vbpy)₃]²⁺ electrodes that have decayed ($\lesssim 30\%$), in HClO₄ electrolyte, restores most of the original electroactivity. More extensively degraded (>80%) electrodes could not be rejuvenated in this way. It seems possible that incorporation of sulfate counterion into these films by repeated poly-[Ru(vbpy)₃]²⁺ \rightarrow poly-[Ru(vbpy)₃]³⁺ conversions may, in the subsequent, repeated reductions, be accompanied by more supporting electrolyte cation (Et₄N⁺) ingress than sulfate egress. This would cause buildup of excess electrolyte in the film, which could retard the transport of electrochemical charge.

Charge-Transport Rates in Poly-[Ru(vbpy)₃]²⁺ Films. A poly-[Ru(vbpy)₃]²⁺ film at, e.g., 1×10^{-8} mol/cm² coverage is ca. 600 Å thick and contains the equivalent of ca. 125 monomolecular layers of [Ru(vbpy)₃]²⁺ units. (With the assumption of a density of 1.35 g/cm³, this corresponds to a site concentration of 1.6 M.) The manner and rate at which the multiple layers of redox sites become oxidized and reduced by the electrode in such a film are of considerable interest. Kaufman and Engler^{17,18} have proposed that electrons can migrate through redox polymers by successive electron-self-exchange reactions between neighbor oxidized and reduced sites (a hopping process, or electron "bucket brigade"). A flow of counterions also occurs to compensate alternations in the electrical charges of the fixed redox sites. The combination

(13) This result generously supplied by K. Willman, The University of North Carolina, 1980.

(14) Umaña, M.; Denisevich, P.; Rolison, D. R.; Nakahama, S.; Murray, R. W. *Anal. Chem.* **1981**, *53*, 1170.

(15) Penn, D. R. *J. Electron Spectrosc. Relat. Phenom.* **1976**, *9*, 29.

(16) (a) Rubenstein, I.; Bard, A. J. *J. Am. Chem. Soc.* **1980**, *102*, 6641. (b) *Ibid.* **1981**, *103*, 5007.

(17) Kaufman, F. B.; Engler, E. M. *J. Am. Chem. Soc.* **1979**, *101*, 547.

(18) Kaufman, F. B.; Schroeder, A. H.; Engler, E. M.; Kramer, S. R.; Chambers, J. Q. *J. Am. Chem. Soc.* **1980**, *102*, 483.

Table II. Exemplary Electrochemical Data for Various Polymers and Copolymers (in 0.1 M Et₄NClO₄/CH₃CN)

electrode	Γ , mol/cm ²	ΔE_p , mV	fwhm, mV	V , mV/s
[Ru(vbpy) ₃] ²⁺				
1	6.1×10^{-10}	15	160	100
2	1.5×10^{-9}	40	175	200
3	5×10^{-9}	30	140	100
4	5×10^{-8}	80	170	50
5	1.3×10^{-7}	80	190	5
6	1.3×10^{-8} ^a	100
[Fe(vbpy) ₃] ²⁺				
7	1.2×10^{-8}	30	175	20
8	2×10^{-8}	70	160	100
9	2×10^{-8}	40	150	50
[Ru(bpy) ₂ (vpy) ₂] ²⁺				
10	1.8×10^{-9}	20	140	50
11	3.1×10^{-9}	40	150	100
12	1.6×10^{-8}	110	200	200
copoly-[[Ru(vbpy) ₃] ²⁺ , [Fe(vbpy) ₃] ²⁺]				
13	5×10^{-9} (Ru)	50	...	100
	5×10^{-9} (Fe)	65	...	
copoly-[[Ru(bpy) ₂ (vpy) ₂] ²⁺ , [Ru(bpy) ₂ (vpy)Cl] ⁺]				
14	6.3×10^{-10}	10	140	100
	3.2×10^{-10} (RuCl)	15	115	

^a Optically transparent SnO₂ electrode. $\Gamma = 1.5 \times 10^{-8}$ mol/cm² by visible spectroscopy, $\lambda_{\max} = 470$ nm.

of ion and electron motions is termed electrochemical charge transport. It has been established^{4,19-25} (and confirmed by a theoretical model²²) that charge transport through redox polymers during their oxidation or reduction obeys electrochemical equations based on Fick's diffusion law. Quantitative charge-transport-rate data in redox polymers are not plentiful and except for poly(vinylferrocene)^{19,20,23} include no instance of a metal complex polymer undiluted by large quantities of dangling uncoordinated ligand.

Cyclic voltammograms of $\leq 10^{-8}$ mol/cm² Pt/poly-[Ru(vbpy)₃]²⁺ electrodes in CH₃CN solvent exhibit Ru^{III/II} currents that vary linearly with potential sweep rate up to 0.2 V/s, the behavior expected when essentially all the poly-[Ru(vbpy)₃]²⁺ sites in the film are oxidized and reduced so rapidly as to remain in Nernstian equilibrium with the electrode at each applied potential. With higher coverage films, peak current increases at a less than linear fashion with potential sweep rate, especially at high sweep rates, and additionally the Ru^{III/II} wave develops "tails" reminiscent of cyclic voltammograms of dissolved reactants^{20b} (compare the low- and high-coverage electrodes, Figure 2C and D, respectively). The peak potential separation ΔE_p also increases in comparison to the small values observed at low coverage (Table II). These phenomena are also observed for thick films of poly-[Fe(vbpy)₃]²⁺ and poly-[Ru(bpy)₂(vpy)₂]²⁺ (Table II) and represent incipient control of the rate of the films' electrochemical reactions by the rate of diffusion of electrochemical charge through the film.

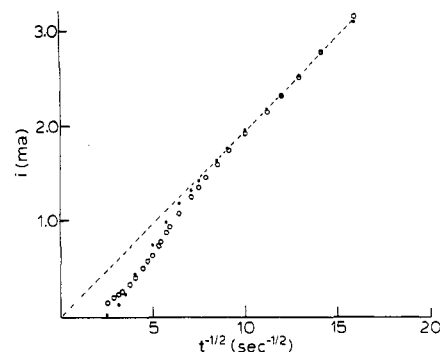


Figure 4. Cottrell plot of current-time curve for 0 \rightarrow +1.7 V vs. SSCE potential step in saturated LiClO₄/CH₃CN at a 7×10^{-9} mol/cm² poly-[Ru(vbpy)₃]²⁺ film on Pt. The slope of the plot, $nFAD_{\text{eff}}^{1/2}C/\pi^{1/2}$, gives $D_{\text{eff}}^{1/2}C = 2.4 \times 10^{-8}$. Open circles are values calculated from finite-diffusion theory¹⁷ for this $D_{\text{eff}}^{1/2}C$.

Potential step chronoamperometry^{20a,26} was used to measure the effective diffusion coefficient D_{eff} for electrochemical charge in the oxidation of a poly-[Ru(vbpy)₃]²⁺ film. Current-time responses for potential steps from 0 to +1.7 V vs. SSCE decay smoothly²⁷ and give linear, short-time Cottrell plots as shown in Figure 4. The drop-off in current at longer times is expected for diffusion in a film of finite thickness and is accurately represented (by open circles on the curve) by finite-diffusion theory previously described.^{20a} The Cottrell slope gives the product $D_{\text{eff}}^{1/2}C = 2.4 \times 10^{-8}$ mol/(cm² s^{1/2}), where C is the concentration in mol/cm³ of [Ru(vbpy)₃]²⁺ sites in the film. Taking $C = 1.6 \times 10^{-3}$ mol/cm³ gives $D_{\text{eff}} = 2.2 \times 10^{-10}$ cm²/s. A similar determination on a different Pt/poly-[Ru(vbpy)₃]²⁺ electrode with $\Gamma = 6 \times 10^{-9}$ mol/cm² gave $D_{\text{eff}}^{1/2}C = 2.1 \times 10^{-8}$ mol/(cm² s^{1/2}) and $D_{\text{eff}} = 1.6 \times 10^{-10}$ cm²/s. It is worth noting that while $D_{\text{eff}}^{1/2}C$ is thought to be fairly reliable, derived D_{eff} values have an uncertainty associated with the film density. Thus, if film density is assumed¹⁴ to be 0.3 g/cm³, D_{eff} is 4.5×10^{-9} and 3.5×10^{-9} cm²/s, respectively.

When the electron-exchange mechanism of Kaufman and Engler is followed,^{17,18} electrons are removed from [Ru(vbpy)₃]²⁺ sites that are remote from the Pt electrode by successive electron transfers between neighbor [Ru(vbpy)₃]²⁺ and [Ru(vbpy)₃]³⁺ sites in the film. The rate at which these electron transfers occur and the rate at which counterions enter the film for charge compensation influence D_{eff} . Translation of D_{eff} into an electron-transfer rate constant is of obvious interest. D_{eff} will be determined by the slowest process limiting charge transport, which may be the intrinsic electron-transfer rate between adjacent sites, which is dictated by the usual vibrational barrier, the rate of charge compensating counterion hopping, which is necessarily coupled to electron transfer, or perhaps the rate of segmental motions of the polymer lattice. The latter could enter the problem through the value of increased orbital overlap in nonequilibrium polymer orientations and/or in structural changes associated with the gain or loss of counterions into the film. We have measured²⁸ the rate at which bromide ions permeate through poly-[Ru(vbpy)₃]²⁺ films; it is $>10^3$ times larger than D_{eff} . Making the reasonable assumption that perchlorate (the counterion in the present

- (19) Daum, P.; Murray, R. W. *J. Electroanal. Chem. Interfacial Electrochem.* **1979**, *103*, 289.
 (20) (a) Daum, P.; Lenhard, J. R.; Rolison, D. R.; Murray, R. W. *J. Am. Chem. Soc.* **1980**, *102*, 4649. (b) Nowak, R. J.; Schultz, F. A.; Umaña, M.; Lam, R.; Murray, R. W. *Anal. Chem.* **1980**, *52*, 315. (c) Daum, P.; Murray, R. W. *J. Phys. Chem.* **1981**, *85*, 389.
 (21) Oyama, N.; Anson, F. C. *J. Electrochem. Soc.* **1980**, *127*, 640.
 (22) Laviron, E. *J. Electroanal. Chem. Interfacial Electrochem.* **1980**, *112*, 1.
 (23) Pearce, P. J.; Bard, A. J. *J. Electroanal. Chem. Interfacial Electrochem.* **1980**, *114*, 89.
 (24) Facci, J.; Murray, R. W. *J. Electroanal. Chem. Interfacial Electrochem.* **1981**, *124*, 339.
 (25) Kuo, K. N.; Murray, R. W. *J. Electroanal. Chem. Interfacial Electrochem.* **1982**, *131*, 37.

- (26) This method is preferred^{20c} over potential sweep voltammetry since compensation for effects of film resistance and possible slow heterogeneous charge transfer²³ is more readily accomplished.
 (27) Distorted, humped current-time curves result, as seen previously,^{20c} when the potential step is insufficiently large to overcome the film's ohmic resistance or the supporting electrolyte concentration is too low. High concentrations of electrolyte apparently drive additional ambient ions into the film to lower its ohmic resistance.
 (28) Ikeda, T.; Schmeil, R.; Denisevich, P.; William, K.; Murray, R. W. *J. Am. Chem. Soc.*, in press.

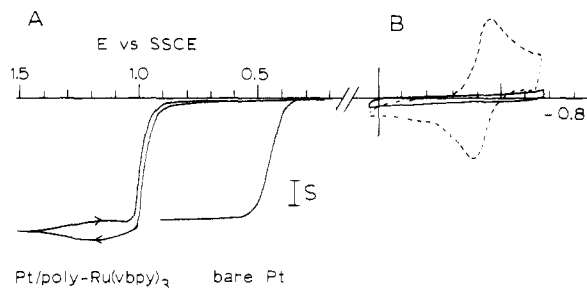


Figure 5. Curve A: rotated Pt-disk electrode voltammetry (2500 rpm) of a 1 mM $[\text{Fe}(\text{bpy})_2(\text{CN})_2]$ solution at a naked Pt and at a 6×10^{-9} mol/cm² poly- $[\text{Ru}(\text{vbpy})_3]^{2+}$ electrode. $S = 25$ and $200 \mu\text{A}/\text{cm}^2$ for curves A and B, respectively. Curve B: cyclic voltammetry at 100 mV/s in 0.1 M $\text{Et}_4\text{NClO}_4/\text{CH}_3\text{CN}$ of a 0.5 mM methylviologen solution at a naked Pt (---) and at a Pt/poly- $[\text{Ru}(\text{vbpy})_3]^{2+}$ (—) electrode.

experiment) has a mobility similar to bromide, we can rule out control of D_{ct} by perchlorate counterion hopping.

The value of D_{ct} represents the rate of *fruitful* "collisions" between neighbor $[\text{Ru}(\text{vbpy})_3]^{2+}$ and $[\text{Ru}(\text{vbpy})_3]^{3+}$ sites. If every "collision" in fact results in electron self-exchange, then the reaction is truly diffusion controlled, D_{ct} represents the diffusion rate, and D_{ct} can be converted to an *effective* electron-transfer rate constant, $k_{\text{ex}}^{\text{app}}$, by using a conventional²⁹ formula for collision-controlled reaction rates. For $D_{\text{ct}} = 2.2 \times 10^{-10}$ cm²/s, 6.9-Å $[\text{Ru}(\text{vbpy})_3]^{2+}$ collision radius,³⁰ and a neglect of electrostatic terms, $k_{\text{ex}}^{\text{app}} = 2.3 \times 10^5 \text{ M}^{-1} \text{ s}^{-1}$ ($k_{\text{ex}}^{\text{app}} = 4.7 \times 10^6 \text{ M}^{-1} \text{ s}^{-1}$ if film density is assumed¹⁴ equal to 0.3 g/cm³). This calculation implicitly assumes that the intrinsic electron-self-exchange rate in the poly- $[\text{Ru}(\text{vbpy})_3]^{2+}$ film exceeds that at which sites collide or otherwise by segmental polymer lattice motions come into proper juxtaposition for electron transfer. It is therefore very interesting that the values for $k_{\text{ex}}^{\text{app}}$ in the film are not very distant from (36- and 1.7-fold, respectively) but are in fact smaller than the self-exchange constant $k_{\text{ex}} = 8.3 \times 10^6 \text{ M}^{-1} \text{ s}^{-1}$ reported³⁰ for freely diffusing $[\text{Ru}(\text{vbpy})_3](\text{ClO}_4)_2$ dissolved in acetonitrile. The comparison suggests that polymer lattice mobility, in this polymer, dominates the rate of charge transport. The difference between $k_{\text{ex}}^{\text{app}}$ and k_{ex} in this comparison is not sufficiently large, however, for the comparison to be completely definitive;³¹ additionally, electrolyte effects in the polymer may differ from those in solution. In a previous^{20a} collision-formula conversion of D_{ct} to $k_{\text{ex}}^{\text{app}}$ for a plasma-polymerized vinylferrocene film, $k_{\text{ex}}^{\text{app}}$ was clearly $\ll k_{\text{ex}}$, and control by the electron-transfer barrier could be more clearly ruled out.

Finally, it is worth noting that D_{ct} in a redox polymer film imposes an upper limit on the rate at which it can oxidize or reduce a chemical substrate in the solution in an electrocatalytic scheme.^{20a,32} With the assumption that the poly- $[\text{Ru}(\text{vbpy})_3]^{2+}$ film is poorly permeable toward the substrate, which is demonstrably²⁸ appropriate for bulky, positively charged metal complex substrates, the maximum flux for a 1×10^{-8} mol/cm² film can be calculated for $D_{\text{ct}} = 2.2 \times 10^{-10}$ cm²/s to be $D_{\text{ct}}C^2/\Gamma_T = 6 \times 10^{-8}$ mol/(cm² s). We have detected the influence of the charge-transport rate on (rapid) cross-electron-exchange reactions involving the poly- $[\text{Ru}(\text{vbpy})_3]^{2+}$ film in a recently completed study;²⁸ analysis of that data produced a value of $D_{\text{ct}}^{1/2}C = 3.4 \times 10^{-8}$ mol/(cm² s^{1/2}),

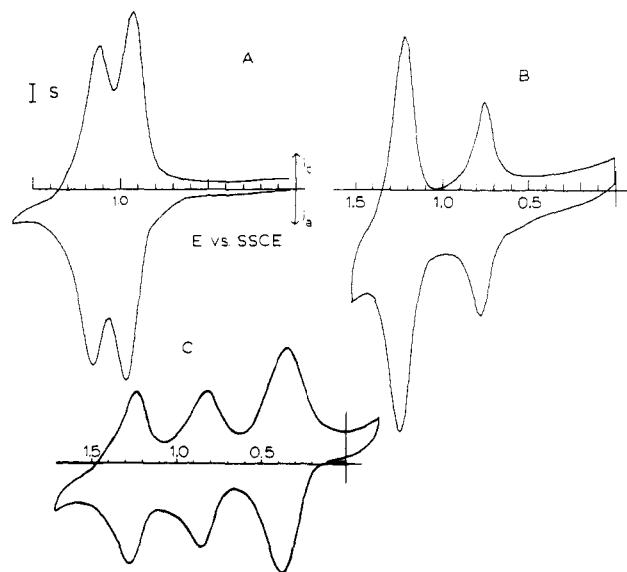


Figure 6. Cyclic voltammetry at 100 mV/s in 0.1 M $\text{Et}_4\text{NClO}_4/\text{CH}_3\text{CN}$ of copolymers on Pt: curve A, 5×10^{-9} , 5×10^{-9} mol/cm² copoly- $[\text{Ru}(\text{vbpy})_3]^{2+}$, $[\text{Fe}(\text{vbpy})_3]^{2+}$ polymerized from a mixture of 0.5 mM $[\text{Ru}(\text{vbpy})_3]^{2+}$ and 1 mM $[\text{Fe}(\text{vbpy})_3]^{2+}$; curve B, 6×10^{-10} , 3×10^{-10} mol/cm² copoly- $[[\text{Ru}(\text{bpy})_2(\text{vpy})_2]^{2+}$, $[\text{Ru}(\text{bpy})_2(\text{vpy})\text{Cl}]^+$] polymerized from a mixture of 0.5 mM $[\text{Ru}(\text{bpy})_2(\text{vpy})_2]^{2+}$ and 2 mM $[\text{Ru}(\text{bpy})_2(\text{vpy})\text{Cl}]^+$; curve C, (50 mV/s) poly- $[[\text{Ru}(\text{bpy})_2(\text{vpy})_2]^{2+}$, $[\text{Ru}(\text{vbpy})_2(\text{CH}_3\text{CN})\text{Cl}]^+$, $[\text{Ru}(\text{vbpy})_2\text{Cl}_2]^{2+}$] polymerized from a mixture of 0.3 mM $[\text{Ru}(\text{bpy})_2(\text{vpy})_2]^{2+}$ and 0.3 mM $[\text{Ru}(\text{vbpy})_2\text{Cl}_2]^{2+}$. $S = 50$, 5, and $8 \mu\text{A}/\text{cm}^2$, respectively, for curves A–C.

in excellent agreement with the experiment of Figure 4.

Polymer Films as Polyelectrolytes and Barriers. Since these polymers are composed of cationic species, they should behave as polyelectrolytes and display ion-exchange properties. Thus, cations in the contacting solution should tend to be excluded from the films whereas anions should be incorporated in them. As shown in Figure 5B, reduction of the methylviologen dication is completely suppressed at Pt/poly- $[\text{Ru}(\text{vbpy})_3]^{2+}$ electrodes. Conversely, a Pt/poly- $[\text{Ru}(\text{bpy})_2(\text{vpy})_2]^{2+}$ electrode soaked in aqueous ferricyanide solution and transferred to clean electrolyte then exhibits a persistent response typical of electrostatically bound ferricyanide.³³

The probably highly cross-linked films of poly- $[\text{Ru}(\text{vbpy})_3]^{2+}$ also display *size exclusion* properties. Both the dication $[\text{Fe}(\text{bpy})_3]^{2+}$ and the neutral $[(\text{bpy})_2\text{Fe}(\text{CN})_2]$ are excluded, whereas the smaller ferrocene molecule readily diffuses through albeit at a slower, membrane-controlled rate. Exclusion of $[(\text{bpy})_2\text{Fe}(\text{CN})_2]$ is illustrated by the rotated-disk-electrode voltammetry of Figure 5A; oxidation of the complex does not occur until potentials generating Ru^{III} -film states are attained, whereupon it is catalytically oxidized. Such size discrimination could provide the basis for selective analytical detection procedures. The exclusion of cations and of relatively large neutral species additionally indicates that the films are free of gross pinhole defects.

Copolymers and Reactive Films. Electropolymerization of these vinyl complexes is readily extended to the preparation of copolymer electrodes. Negative-potential scanning in a solution containing 0.2 mM $[\text{Ru}(\text{vbpy})_3]^{2+}$ and 0.4 mM $[\text{Fe}(\text{vbpy})_3]^{2+}$ yields a polymer film containing both the ruthenium and iron species (Figure 6A). The two cyclic voltammetric waves occur at the same potentials as for individual homopolymer films of these monomers, and the copolymer response is a simple addition of the electrochemical responses of monomers. This copolymer furthermore has been shown by angular emission XPS to be randomly mixed.⁸

(29) Hammes, G. G. "Principles of Chemical Kinetics"; Academic Press: New York, 1978; p 62.

(30) Chan, M. S.; Wahl, A. C. *J. Phys. Chem.* **1978**, *82*, 2543.

(31) (a) Also, if we assume that the electron transfer is itself the slow step, then with^{43b} $D_{\text{ct}} = \pi k_{\text{ex}}^{\text{app}} C^2/4$, $k_{\text{ex}}^{\text{app}} = 6.6 \times 10^6 \text{ M}^{-1} \text{ s}^{-1}$. This is also close to the solution value. (b) Ruff, I.; Friedrich, V. G. *J. Phys. Chem.* **1971**, *75*, 3297.

(32) Rocklin, R. D.; Murray, R. W. *J. Phys. Chem.* **1981**, *85*, 2104.

(33) Oyama, N.; Anson, F. C. *J. Electrochem. Soc.* **1980**, *127*, 247.

Similarly, reduction of a mixture of $[\text{Ru}(\text{bpy})_2(\text{vpy})_2]^{2+}$ and $[\text{Ru}(\text{bpy})_2(\text{vpy})\text{Cl}]^+$ gives a copolymer (Figure 6B) with $\text{Ru}^{\text{III/II}}$ waves at potentials expected for the individual monomers (Table I). Analogous additive responses have been reported by Oyama and Anson^{2b} for a polymer-mixture film. In general, one can probably expect such behavior whenever the individual copolymer components are reasonably randomly mixed and have sufficient populations of nearby, like neighbors to permit efficient charge transport to the Pt electrode by the usual electron-self-exchange process. If the neighbor population of one component is too low, however, it can conceivably react slowly enough that electron mediation by the majority host complex becomes important (vide infra).

It has not been possible to form significantly thick homopolymer films of poly- $[\text{Ru}(\text{bpy})_2(\text{vpy})\text{Cl}]^+$. Reducing this monomer at a potential (-1.64 V vs. SSCE) beyond its first (reversible) reduction wave (Table I) yields very low coverage films ($\sim 10^{-10}$ mol/cm²), with a somewhat broad $\text{Ru}^{\text{III/II}}$ wave at +0.76 V. Reduction beyond the second, irreversible ($i_p \approx 0$) wave of the monomer deposits more polymer ($\sim 10^{-9}$ mol/cm²), but in the process an acetonitrile ligand is apparently substituted for the chloride, giving a well-formed $\text{Ru}^{\text{III/II}}$ wave at +1.29 V vs. SSCE. A similar reactivity pattern is observed for $[\text{Ru}(\text{bpy})_2(\text{py})\text{Cl}]^+$ solutions in acetonitrile.

Polymerization of the monomer *cis*- $\text{Ru}(\text{vbpy})_2\text{Cl}_2$ is of interest because its films might be useful synthetic precursors to other films. However, reduction of its solutions at -1.5 V gave a polymer film with three $\text{Ru}^{\text{III/II}}$ waves, at ca. +0.3 (small), +0.83 (predominant), and +1.35 V vs. SSCE, with small overall coverage ($\sim 10^{-9}$ mol/cm²), whereas reduction at -1.7 V produced a film with only the last two $\text{Ru}^{\text{III/II}}$ waves, that at +1.35 V now predominating. Tentatively, we assign these waves to copolymer constituents $[\text{Ru}(\text{vbpy})_2\text{Cl}_2]$, $[\text{Ru}(\text{vbpy})_2(\text{CH}_3\text{CN})\text{Cl}]^+$, and $[\text{Ru}(\text{vbpy})_2(\text{CH}_3\text{CN})_2]^{2+}$, respectively, the latter two resulting from ligand replacement as above.

As with $[\text{Ru}(\text{bpy})_2(\text{vpy})\text{Cl}]^+$, it is easier to obtain intact poly- $[\text{Ru}(\text{vbpy})_2\text{Cl}_2]$ sites in a copolymer with $[\text{Ru}(\text{bpy})_2(\text{vpy})_2]^{2+}$. Reduction of a mixture of these complexes at -1.35 V vs. SSCE produced in one trial a film with two $\text{Ru}^{\text{III/II}}$ waves, at +0.30 and +1.26 V, as expected for poly- $[\text{Ru}(\text{vbpy})_2\text{Cl}_2]$ and poly- $[\text{Ru}(\text{bpy})_2(\text{vpy})_2]^{2+}$ sites, respectively, and in another trial, illustrated in Figure 6C, some substitution occurred to produce also a third wave at +0.84 V, for poly- $[\text{Ru}(\text{vbpy})_2(\text{CH}_3\text{CN})\text{Cl}]^+$. This Pt/poly- $[\text{Ru}(\text{vbpy})_2\text{Cl}_2]-[\text{Ru}(\text{vbpy})_2(\text{CH}_3\text{CN})\text{Cl}]^+ - [\text{Ru}(\text{bpy})_2(\text{vpy})_2]^{2+}$ polymer film electrode exemplifies a modified electrode surface bearing more than two electrochemically distinct redox constituents. Copolymerization is a promising approach for preparing modified electrodes with bandlike surface states and thus potentially generalized outer-sphere electrocatalytic properties. For example, the electrode in Figure 6C could in principle, by choice of electrode potential, mediate the electrooxidation of one, two, or three (or more) substrate constituents of the solution.

Ruthenium nitro complexes have been of interest to us both in solutions³⁴ and as immobilized monolayers³⁵ on electrodes, owing to their reactivity in a disproportionation reaction, their acid-base chemistry, and, as $\text{Ru}^{\text{III}}\text{NO}_2$, their usefulness as oxygen-transfer catalysts toward triphenylphosphine. A detailed mechanistic study of immobilized $[\text{Ru}(\text{bpy})(i\text{-nic})\text{NO}_2]^+$ (*i-nic* = isonicotinic acid) shows^{35a} that the oxidized complex linkage isomerizes rapidly and reversibly, to the O-bound

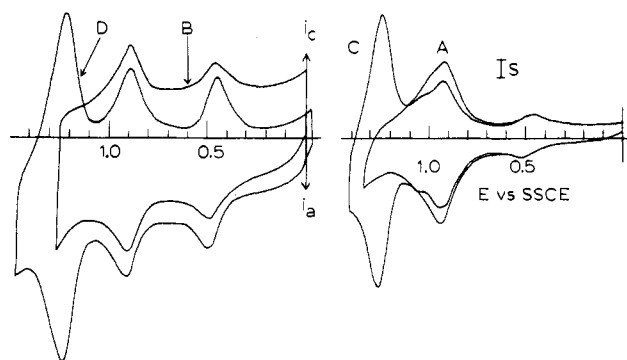


Figure 7. Cyclic voltammetry at 200 mV/s in 0.1 M $\text{Et}_4\text{NClO}_4/\text{CH}_3\text{CN}$ of high-coverage (curve A) and low-coverage (curve B) Pt/poly- $[\text{Ru}(\text{bpy})_2(\text{vpy})\text{NO}_2]^+$ electrodes after extensive cycling leading to decay of the RuNO_2 function; curves C and D are similarly decayed high and low coverage, respectively, Pt/copoly- $[[\text{Ru}(\text{bpy})_2(\text{vpy})_2]^{2+}, [\text{Ru}(\text{bpy})_2(\text{vpy})\text{NO}_2]^+]$. $S = 2.5, 0.25, 2.5,$ and $0.5 \mu\text{A}$ for curves A-D, respectively.

(nitrito) Ru^{III} complex, and on a much longer time scale reacts irreversibly by two competing reactions paths to yield a mixture of nitrosyl and nitrate complexes, with the latter predominating. We were interested in whether the latter reactivity pattern would be altered in a polymeric form of the ruthenium nitro complex.

$[\text{Ru}(\text{bpy})_2(\text{vpy})\text{NO}_2]^+$ could be polymerized to films with modest coverages by potentiostating past either the first (-1.45 V) or the second (1.69 V) reduction waves. (In the latter case, some ligand substitution by acetonitrile occurs.) When the Pt/poly- $[\text{Ru}(\text{bpy})_2(\text{vpy})\text{NO}_2]^+$ electrodes are placed in clean supporting electrolyte and the potential is repeatedly cycled between 0 and +1.4 V, the wave for the $\text{Ru}^{\text{III/II}}\text{NO}_2$ couple ($E^{\circ}_{\text{surf}} = +1.02$ V vs. SSCE) gradually decreases while waves at potentials characteristic of the nitrate (+0.92 V) and nitrosyl (+0.47 V) complexes grow in. This pattern, in which the nitrate complex is the predominant (Figure 7A) ultimate product, is very reminiscent of that observed³⁵ for alkylaminesilane-immobilized $[\text{Ru}(\text{bpy})_2(i\text{-nic})\text{NO}_2]^+$. Lower coverage Pt/poly- $[\text{Ru}(\text{bpy})_2(\text{vpy})\text{NO}_2]^+$ electrodes, on the other hand, consistently produce, after decay to products, more nearly equal amounts of the nitrosyl and nitrate complexes (Figure 7B). Furthermore, at high coverages, careful inspection shows that the nitrosyl wave reaches its maximum size before the nitrate and nitro waves cease changing. These results show that $\text{Ru}^{\text{III}}\text{NO}_2$ reactivity is changed by the polymeric environment. Since the nitrosyl complex is bimolecularly produced, probably by a $\text{Ru}^{\text{III}}\text{NO}_2 + \text{Ru}^{\text{III}}\text{ONO}$ reaction, the results suggest that only a small fraction of pairs of complex sites are able to rapidly achieve proper relative orientation for disproportionation to equal amounts of nitrosyl and nitrate products. The other sites are competitively converted by an as yet nonunderstood reaction directly to the nitrate complex.

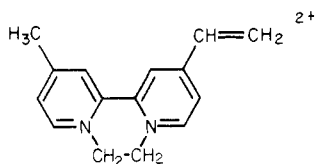
Homogeneous experiments³⁵ have suggested that the presence of excess oxidant (e.g., $[\text{Ru}(\text{bpy})_3]^{3+}$) can enhance production of the nitrate complex from $\text{Ru}^{\text{III}}\text{NO}_2$. We accordingly copolymerized $\text{Ru}(\text{bpy})_2(\text{bpy})\text{NO}_2^+$ with $\text{Ru}(\text{bpy})_2(\text{vpy})_2^{2+}$. As shown in Figure 7C and D (the former complex is in excess in the copolymer), the nitrate/nitrosyl mixture obtained after cycling through the $\text{Ru}^{\text{III/II}}$ waves to allow $\text{Ru}^{\text{III}}\text{NO}_2$ reaction remains ~ 1 at low coverages and is $\gg 1$ at higher coverage.

Scope and Mechanism of the Polymerization. Our original hypothesis⁸ for electropolymerization of these complexes was based on the known anionic polymerization of vinylpyridine and the nature of the $[\text{Ru}(\text{bpy})_3]^{2+}$ reductions (ligand localized), that the transfer of negative charge to a vinyl substituent

(34) Keene, F. R.; Salmon, D. J.; Meyer, T. J. *J. Am. Chem. Soc.* **1977**, *99*, 2384.

(35) (a) Abruña, H. D.; Walsh, J. L.; Meyer, T. J.; Murray, R. W. *Inorg. Chem.* **1981**, *20*, 1481. Abruña, H. D.; Walsh, J. L.; Meyer, T. J.; Murray, R. W. *J. Am. Chem. Soc.* **1980**, *102*, 3272.

on a reduced ruthenium vinylpyridine or bipyridine complex might lead to polymerization. Operationally, polymerization occurs; the available data are qualitatively consistent with the hypothesis. The vinyl-substituted complexes listed in Table I all form polymeric, electroactive films. Polymerization is aided (where comparison is possible without other interfering chemistry) by two-electron as opposed to one-electron reduction. The complex $[\text{Ru}(\text{bpy})_2(\text{acrylonitrile})_2]^{2+}$ can be polymerized, albeit poorly, by potentiostating at -1.77 V, whereas the related complex $[\text{Ru}(\text{bpy})_2(\text{allylamine})_2]^{2+}$, which has interrupted conjugation between the metal center and the vinyl group, forms no polymeric film even upon prolonged electrolysis. The polymerization of $[\text{Ru}(\text{vbpy})_3]^{2+}$ or $[\text{Ru}(\text{bpy})_2(\text{vpy})_2]^{2+}$ is not peculiar to acetonitrile solvent (it can be effected in 1,2-dimethoxyethane and CH_2Cl_2), the electrode substrate (Pt, carbon, SnO_2 , and TiO_2 all work), or the complexed metal ($[\text{Fe}(\text{vbpy})_3]^{2+}$ can be polymerized). Reductive polymerizations of $[\text{Co}(\text{vbpy})_3]^{3+}$ and $[\text{Cr}(\text{vbpy})_3]^{3+}$ have been attempted; a film forms on the electrode, but it is not electroactive. These reduced complexes are apparently too labile, and the metal is lost. Finally, the closely related vinyl monomer "vinyl-diquat", VDQ^{2+}



is readily polymerized³⁶ by two-electron reduction at ca. -1.00 V vs. SSCE. This polymerization is patently a "ligand-centered" case.

There is also evidence that the polymerization involves, at least in part, a chain-propagating step. As we have reported⁵, $[\text{Ru}(\text{bpy})_2(\text{vpy})\text{Cl}]^+$ is not reduced nor does it form a polymer at -1.37 V, but reduction of $[\text{Ru}(\text{bpy})_2(\text{vpy})_2]^{2+}$ in the presence of $[\text{Ru}(\text{bpy})_2(\text{vpy})\text{Cl}]^+$ nonetheless incorporates the latter complex into the copolymer film. The copolymer film of Figure 6B was in fact formed in such an experiment. We have now found a similar result in copolymerizing $[\text{Ru}(\text{vbpy})_2\text{Cl}_2]$ with $[\text{Ru}(\text{bpy})_2(\text{vpy})_2]^{2+}$, where reduction at -1.35 V incorporates the former complex into the copolymer although it is not reduced at that potential. The terpolymer in Figure 6C was produced in this manner. On the other hand, this is not a completely general effect since reduction of VDQ^{2+} monomer at -1.0 V in the presence of $[\text{Ru}(\text{vbpy})_3]^{2+}$ monomer (the latter is not reduced) incorporates no $[\text{Ru}(\text{vbpy})_3]^{2+}$ copolymer into the film formed.³⁶

It is difficult to obtain meaningful quantitative information on the polymerization efficiency. For example, a Pt electrode was briefly held at -1.3 mV in a solution of $[\text{Ru}(\text{bpy})_2(\text{vpy})_2]^{2+}$, the charge passed was measured and the electrode was disconnected and allowed to stand quietly in the solution for 20 min. The subsequently measured polymer film coverage accounted for only 5–10% of the original cathodic charge passed. In an efficient chain mechanism, coverage could greatly exceed the polymerization initiating charge. The situation is complex, however, in that the rate of the polymerization reaction is coupled to the rates of mass transfer of monomer to the electrode and of reduced monomer away from the electrode, of conproportionation of (two-electron) reduced monomer with fresh monomer in the diffusion layer, and of eventual oxidation of the electrode film (by electron exchange with monomer or with impurities like trace dioxygen), which terminates polymerization. Furthermore we measure only the polymer that remains on the electrode, and the Teflon collar

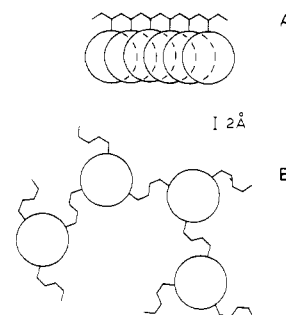


Figure 8. To-scale schematic drawing of poly- $[\text{Ru}(\text{vbpy})_3]^{2+}$ assuming linear (A) vinyl coupling and dimer-bridge (B) vinyl coupling. In curve A, steric crowding should cause spiraling of $[\text{Ru}(\text{vbpy})_3]^{2+}$ units around the chain axis.

coloration shows that this is an incomplete measure. Soluble oligomers may also form in the solution as evidenced by a slightly red-shifted λ_{max} , and with long deposition times or stirred solutions, particulate polymer can be observed in the cell. For these reasons, the low percentage of charge passed that results in film formation is not interpretable in a simple fashion.

Relative film-forming efficiencies for polymerization of different monomers suffer less from the above caveats and provide some meaningful insights. As a general rule, ruthenium complexes bearing only one vinyl substituent deposit poorly. This, the complex $[\text{Ru}(\text{bpy})_2(\text{vbpy})]^{2+}$ yields low-coverage electrodes ($\sim 5 \times 10^{-10}$ mol/cm²) even upon prolonged electrolysis, as does the complex $[\text{Ru}(\text{bpy})_2(\text{vpy})\text{Cl}]^+$. Polymer films deposited from $[\text{Ru}(\text{bpy})_2(\text{vpy})\text{NO}_2]^+$ are only about 2 times thicker, whereas films from $[\text{Ru}(\text{vbpy})_3]^{2+}$, $[\text{Fe}(\text{vbpy})_3]^{2+}$, and $[\text{Ru}(\text{bpy})_2(\text{vpy})_2]^{2+}$ are $>10^2$ times thicker. Much larger quantities of monovinyl monomers can be deposited by the copolymer method described above. Significantly, in copolymerizations of $[\text{Ru}(\text{bpy})_2(\text{vpy})_2]^{2+}$ with $[\text{Ru}(\text{bpy})_2(\text{vpy})\text{Cl}]^+$, or $[\text{Ru}(\text{bpy})_2(\text{vbpy})]^{2+}$ with $[\text{Fe}(\text{vbpy})_3]^{2+}$, and of $[\text{Ru}(\text{bpy})_2(\text{vpy})_2]^{2+}$ with $[\text{Ru}(\text{bpy})_2(\text{vpy})\text{NO}_2]^+$, the monovinyl monomer never comprises more than 50% of the copolymer film even though the reaction mixture contains a great deficiency of the other constituent (by as much as 1/10).

In view of the above results, we suggest that the reluctance of monovinyl complexes to polymerize is steric in origin. The repeated addition of monomer units to a growing polyvinyl backbone requires the close approach of the very bulky bipyridine complexes as illustrated in the schematic, to-scale diagram in Figure 8A. Linear chain growth requires (sterically) a helical spiral with little flexibility. The monovinyl analogue VDQ^{2+} (vide supra) is sterically much less bulky and can be polymerized to larger coverages.³⁶ If two or more vinyl groups are present in the metal complex monomer, on the other hand, a polymerization need *in the limit* involve only the coupling of two vinyl groups in a chain with subsequent units attaching themselves to the other vinyl groups of the monomer (Figure 8B). In this manner the monovinyl $[\text{Ru}(\text{bpy})_2(\text{vbpy})]^{2+}$ would self-propagate poorly but could readily in a mixture add to the "dangling" vinyl groups in a poly- $[\text{Ru}(\text{vbpy})_3]^{2+}$ network. The possibility that polymerization in the manner of Figure 8B represents a significant fraction of the total polymer coupling makes it inappropriate to refer to these polymers as "fully metalated poly(vinylpyridine) or poly(vinylbipyridine)" polymers, since many vinylbipyridine units may actually exist as dimers. A more accurate structural description of such sites in the polymer would be as ruthenium cluster complexes held together with bridging ligands. Finally, we should note that if ligands on reduced $[\text{Ru}(\text{vbpy})_3]^0$ have radical anion character, their dimer coupling as activated olefins^{37–39} should be tail-to-tail as drawn in Figure 8B.

(36) Willman, K.; Murray, R. W. *J. Electroanal. Chem. Interfacial Electrochem.*, in press.

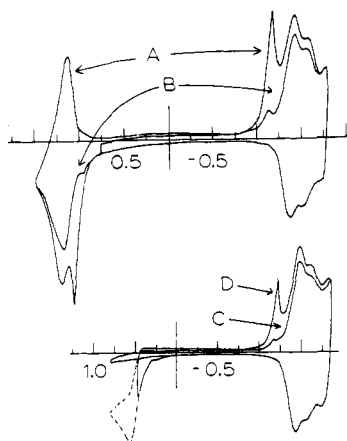


Figure 9. Cyclic voltammetry at 100 mV/s in 0.1 M Et₄NClO₄/CH₃CN of a Pt/poly-[Ru(vbpy)₃]²⁺ electrode: curve A, potential scans between +1.5 and -1.8 V vs. SSCE; curve B, potential scans between +0.75 and -1.8 V showing absence of trapping/untrapping peaks after initial scans through only the anodic M^{II/III} and the cathodic M^{II/0} waves, respectively; curve C, scan between +0.42 and -1.8 V showing absence of trapping/untrapping peaks; curve D, 1 mM added ferrocene (gives anodic peak at +0.5 V), with potential held 30 s at +0.42 V and then scanned to -1.8 V, making trapping/untrapping peaks appear at ca. -1.2 V.

Coupling of this nature is known for vinylpyridine radical anions^{40,41} and can in the absence of proton sources be followed by chain growth.⁴² Further structural work is needed to assess the merits of the above analogy.

It is important to note that the polymerizations described here do not result in electrode passivation as is typical of most electropolymerizations. That is, reduction of a Pt/poly-[Ru(vbpy)₃]²⁺ film electrode to Pt/poly-[Ru(vbpy)₃]⁰ provides an electron-rich surface⁴³ that is just as effective at reducing fresh [Ru(vbpy)₃]²⁺ monomer as is a naked Pt electrode. This of course must be the mechanism by which thick films of poly-[Ru(vbpy)₃]²⁺ are produced since evidence presented above shows that large cations do not penetrate the polymer films. Additionally, unreacted vinyl substituents of the outermost poly-[Ru(vbpy)₃]²⁺ sites are viewed as capable of coupling with fresh monomer so that even though previous polymerization was halted by oxidizing the film (as by scanning electrode potential positively), polymerization can be reinitiated by rereducing the film, which reduces and binds further monomer sites to thicken the film. Many of these nonpassivating characteristics are also found in the electropolymerization of pyrroles described by Diaz and co-workers⁴⁴ although the polymerization chemistry and polymers formed are quite different from those described here.

Charge-Trapping Features of the Film. Cyclic voltammograms of poly-[Ru(vbpy)₃]²⁺, poly-[Ru(bpy)₂(vpy)₂]²⁺, and poly-[Fe(vbpy)₃]²⁺ electrodes show sharp prewaves near the M^{3+/2+} couples and the bipyridine reductions (Figure 9A).

The magnitude of these spikes depends on electrode history. If, during the deposition process, the potential is cycled between M^{III/II} and bipyridine reduction regions (instead of only between 0 V and the bipyridine reductions), the prewaves become much more prominent. When conventionally prepared electrodes are cycled in clean supporting electrolyte over the entire potential range, the prewaves also gradually increase. The presence of these features is not the result of impurities in solvent or supporting electrolyte nor does it depend on the nature of the electrode substrate: the prewaves are seen in CH₃CN/Et₄NClO₄, CH₂Cl₂/Bu₄NClO₄, and CH₃CN/LiClO₄ and on Pt, C, Au, and SnO₂ electrodes. Moreover, since the [Ru(bpy)₂(vpy)₂]²⁺ and [Fe(vbpy)₃]²⁺ complexes have no common precursors, the prewaves cannot reflect a contaminant from their preparation. It appears that these spikes are associated with a chemical degradation of the reduced polymer, perhaps by traces of oxygen or its reduction products.

The cyclic voltammetric behavior of the prewaves is strikingly similar to that of bilayer electrodes described elsewhere.^{8,45} The potentials of the current spikes shift with scan rate, moving closer to the main waves at faster sweep rates. As the magnitudes of the prewaves increase during "abnormal" deposition conditions, they also shift toward the main waves. As with bilayer electrodes, the spikes behave as *trapped oxidation states*: if after a spike and its associated main wave have been scanned through and back, the potential sweep is reversed before the other spike is reached, the original spike is greatly attenuated (Figure 9B). Thus the pair of prewaves seem to represent the anodic and cathodic branches of the same redox couple. We suggest, therefore, that they are associated with *isolated* sites of damaged polymer. Such sites apparently are too immobile and/or too dilute to react with the platinum surface and can undergo electron transfer only by mediation via poly-[Ru(vbpy)₃]²⁺ sites in the bulk of the polymer. This is similar to the process operating in deliberately physically segregated bilayer electrodes.

Although the identity of the species involved in these prewaves remains unknown at this point, the use of mobile solution redox species provides some information. For example, the cyclic voltammogram of a Pt/poly-[Ru(vbpy)₃]²⁺ electrode immersed in a solution of ferrocene is shown in Figure 9C. Here after an initial negative-potential excursion (curve C), the electrode potential is held briefly at +0.42 V, near the leading edge of the ferrocene oxidation. Then, when a second negative scan (Figure 9D) is conducted, the cathodic prewave is restored to nearly its original height, without the potential ever having been scanned into the anodic prewave. Thus ferrocenium ions generated within the film at +0.35 V have chemically oxidized the reduced trapped sites. This result shows that the *E*^o of whatever species is responsible for this prewave is more negative than ca. +0.4 V (*E*^o for the ferrocenium/ferrocene couple). Further efforts of this sort to establish the approximate redox potential and identity of the prewave species are in progress.

Acknowledgment. Helpful discussions with Professor M. Baizer and K. W. Willman and XPS spectroscopy by Dr. M. Umaña are gratefully acknowledged. This research was supported in part by grants from the National Science Foundation. This is paper 38, in a series on chemically modified electrodes.

Registry No. [Ru(vbpy)₃]²⁺, 75675-24-0; [Fe(vbpy)₃]²⁺, 75675-26-2; [Ru(bpy)₂(vpy)₂]²⁺, 75687-40-0; [Ru(bpy)₂(vpy)Cl]⁺, 75675-25-1; Ru(vbpy)₂Cl₂, 80864-60-4; [Ru(bpy)₂(vpy)NO₂]⁺, 80864-61-5; [Ru(bpy)₂(vbpy)]²⁺, 74171-78-1; [Ru(bpy)₂(MeCN)vpy]²⁺, 80864-62-6; [Ru(vbpy)₂(MeCN)₂]²⁺, 80864-63-7; [Ru(vbpy)₂(CH₃CN)Cl]⁺, 80864-64-8.

- (37) Szwarc, M. "Carbanions, Living Polymers, and Electron Transfer Processes"; Interscience: New York, 1968; p 367.
 (38) Baizer, M. M. "Organic Electrochemistry"; Baizer, M. M., Ed.; Marcel Dekker: New York, 1973; pp 679-704.
 (39) Puglisi, V. J.; Bard, A. J. *J. Electrochem. Soc.* **1972**, *119*, 829.
 (40) Anderson, J. D.; Baizer, M. M.; Prill, E. J. *J. Org. Chem.* **1965**, *30*, 1645.
 (41) Lee, C. L.; Smid, J.; Szwarc, M. *Trans. Faraday Soc.* **1963**, *59*, 1192.
 (42) Baizer, M. M.; Anderson, J. D. *J. Org. Chem.* **1965**, *30*, 1351.
 (43) Although the outer boundary of the Pt/poly-[Ru(vbpy)₃]⁰ surface acts as an electrode, reducing [Ru(vbpy)₃]²⁺ monomer there, this is a simply a case of electron-transfer mediation. Thus the poly-[Ru(vbpy)₃]^{2+/0} film should not be regarded as an electronic conductor, since it conducts electrons by the fundamentally different process of internal electron-self-exchange reactions.
 (44) Kanazawa, K. K.; Diaz, A. F.; Geiss, R. H.; Gill, W. D.; Kwak, J. F.; Logan, J. A.; Rabolt, J. F.; Streit, J. B. *J. Chem. Soc., Chem. Commun.* **1979**, 854.

- (45) Denisevich, P.; Willman, K.; and Murray, R. W. *J. Am. Chem. Soc.* **1981**, *103*, 4727.